JETIR.ORG ISSN: 2349-5162 | ESTD Year : 2014 | Monthly Issue
JOURNAL OF EMERGING TECHNOLOGIES AND INNOVATIVE RESEARCH (JETIR)
An International Scholarly Open Access, Peer-reviewed, Refereed Journal

Theoretical Study of Isatin and its Halogenated Derivatives

Esha Arora

Department of Chemistry, Shyama Prasad Vidyalaya Lodhi Estate, New Delhi 110003

Abstract

The comprehensive study of isatin and its halogenated derivatives elucidates the multifaceted impact of halogenation on isatin and its derivatives, spanning from stability and electronic transitions to reactivity and vibrational properties. The study, focusses on their relative stability, electronic transitions, NMR chemical shifts, UV-Vis spectroscopy, thermochemistry, global reactivity parameters, and vibrational spectra.The findings demonstrate that specific halogen substitutions can significantly influence the stability, electronic structure, optical properties, thermochemistry, and reactivity of isatin derivatives. These insights could be invaluable for the design and development of new materials and pharmaceuticals based on isatin, highlighting the potential for targeted modifications to achieve desired properties.

Keywords: NBO (Natural Bond Orbital) analysis, Chemical shifts, UV-Vis spectroscopy, Thermochemistry, Keto-enol tautomerism, Conformational isomerization, Global Reactivity Parameters, Vibrational spectra, Hyperconjugative effect, Resonance effect, Molecular stability, Electronic transitions, Thermodynamic feasibility

1. Introduction

The biological activities of isatin and its derivatives have been known for a long time.Isatin derivatives have several important pharmaceuticals and medicinal properties including anticancer, anti-HIV, antiviral, antitumor, antifungal, antimalarial, antioxidant, anti-inflammatory, antimicrobial, analgesics, anticonvulsants and so on[1-11].The isatin also possess neuroprotective properties, therefore they can be used in treating diseases like Alzheimer's and Parkinson's disease[12,13].Fluorosubstituted isatin derivative, was approved by the FDA (U.S. Food and Drug Administration) for treatment of advanced renal cell carcinoma [14] which indicates the important use of halogen in the drug discovery and development.

Introduction of halogen in isatin increases lipophilicity which leads to greater permeability to lipid membranes coupled with increase in central molecule biological activity due to its electronegativity which results in enhanced binding, metabolic stability, selectivity and improved physicochemical properties [15,16].

Therefore, it is worthwhile to study molecular properties of halogen substituted isatin derivatives and its relation to medicinal properties.

2. Computational Details

Two enol conformers viz. enol1 and enol2 and one keto conformer(Figure 1)are explored for relative energy calculations of isatin and halogen substitutedisatin compounds in gas phase. The numbering scheme of the isatin and its halogen derivatives is shown in Figure 1.The geometry optimized tautomers and conformers of isatin and its various halogen derivatives are shown inFigure 2.In order to know the most stable conformer of these tautomers, we geometry optimized all the structures using density functional B3LYP/6-311++G** [17-19] calculations, and then we performed vibrational analysis for each final optimized structure which revealed no imaginary frequencies. The vibrational frequencies were scaled by a factor of 0.9679 andand zero-point energies scaled by a factor of 0.9877 and added to the calculated energies to give total energy [20].Thermodynamic properties such as enthalpies, and Gibbs energies were calculated at 298.15 K and 1 atm pressure. The NBO (Natural Bond Orbital) [21]analysis was performed in order to understand charge transfer within the molecule.

UV-Vis spectra were calculated using the Time-Dependent DFT (TD-DFT) approach [22-24] in DMSO solvent.All computations were performed using the Gaussian 09 packages[25].

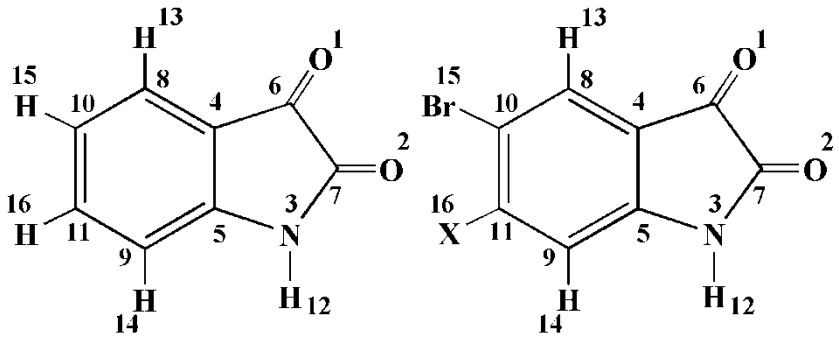

1a 1b

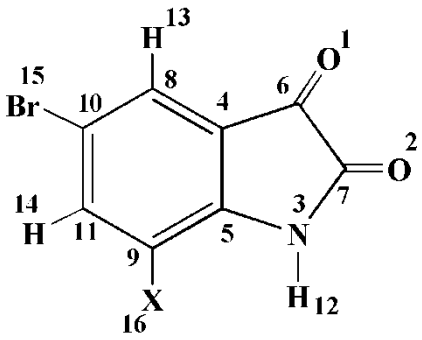

1c

Figure 1 Numbering scheme of Isatin (1a), 10-Bromo-11-haloisatin (1b), 10-Bromo-9-haloisatin (1c)

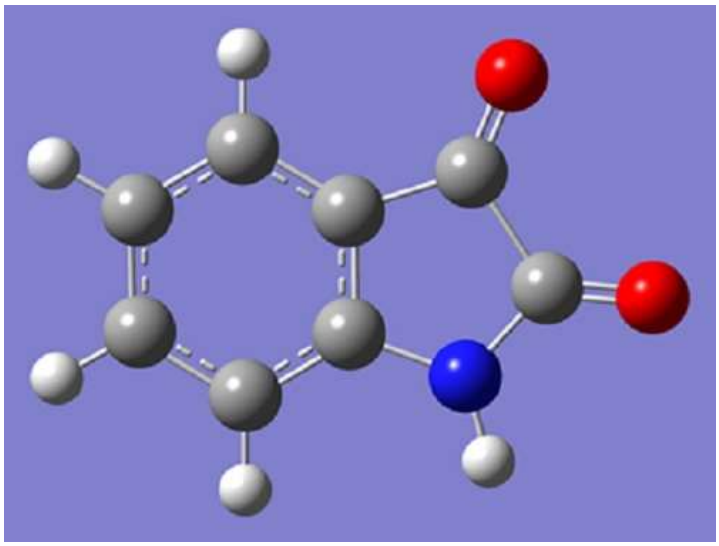	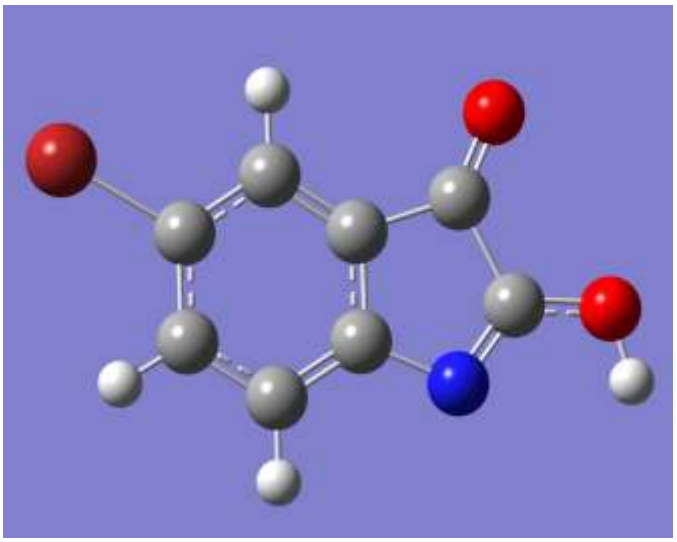
IST (KETO)	**IST (ENOL1)**
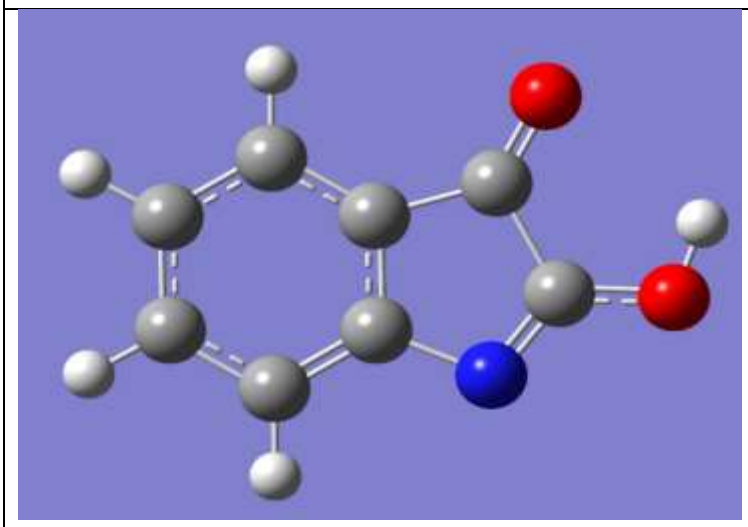	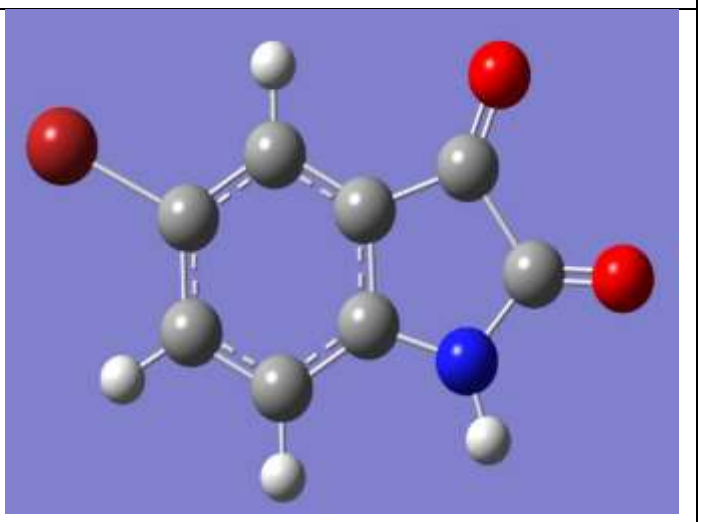
IST (ENOL2)	**IST-10 (KETO)**
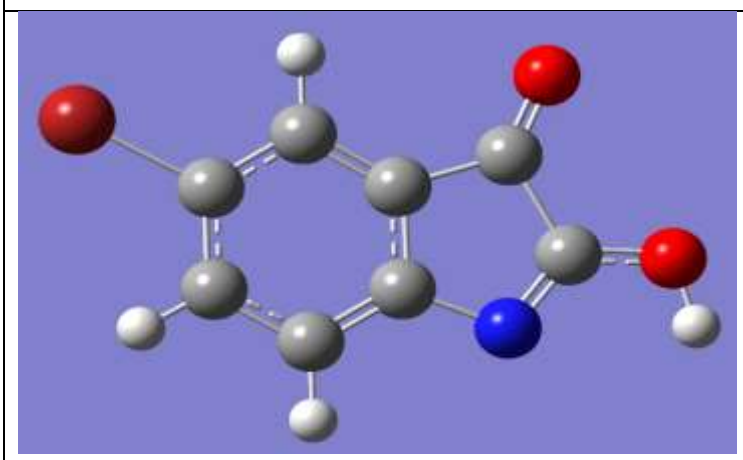	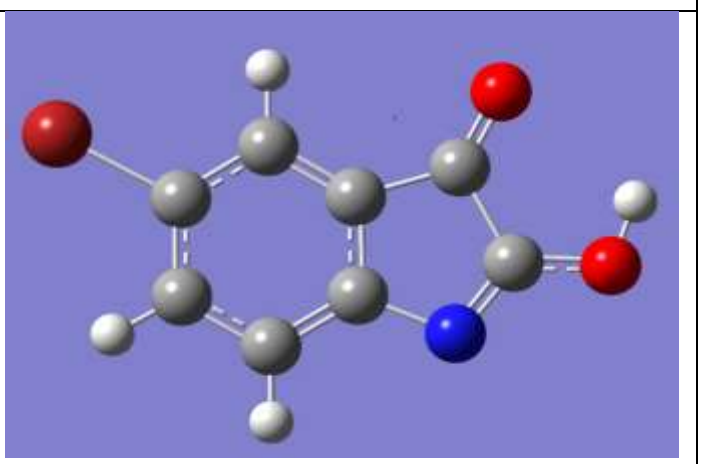
IST-10 (ENOL1)	**IST-10 (ENOL2)**

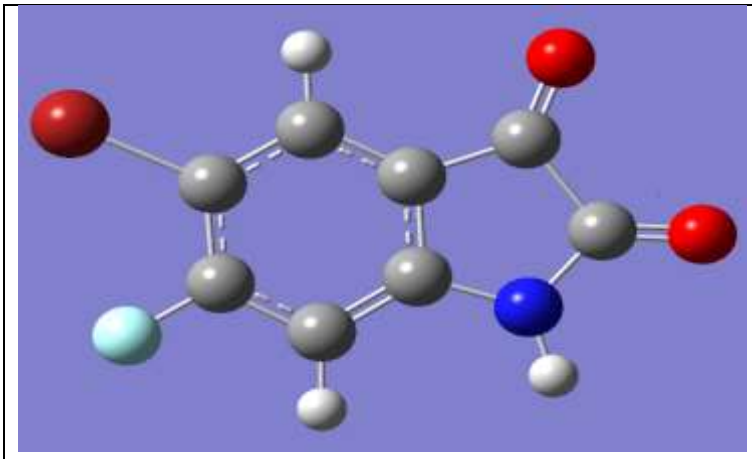	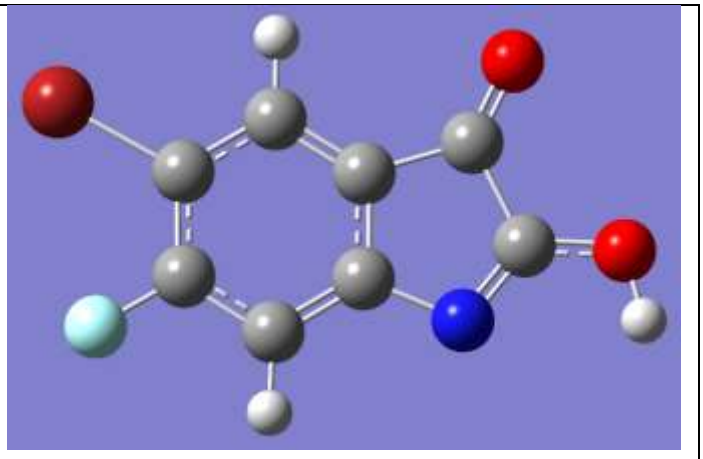
IST-10A (KETO)	**IST-10A (ENOL1)**
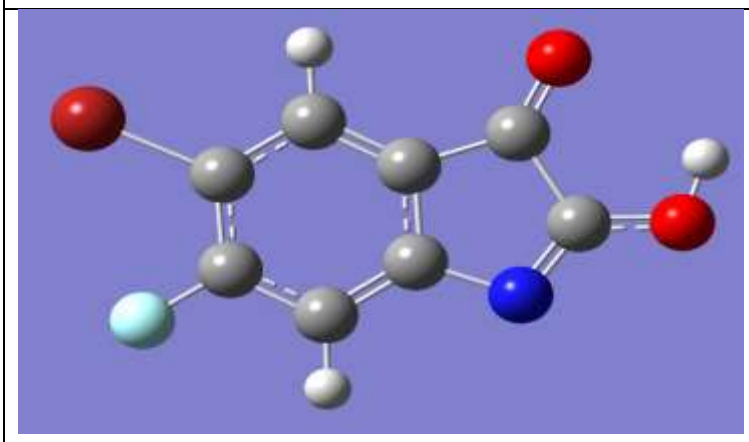	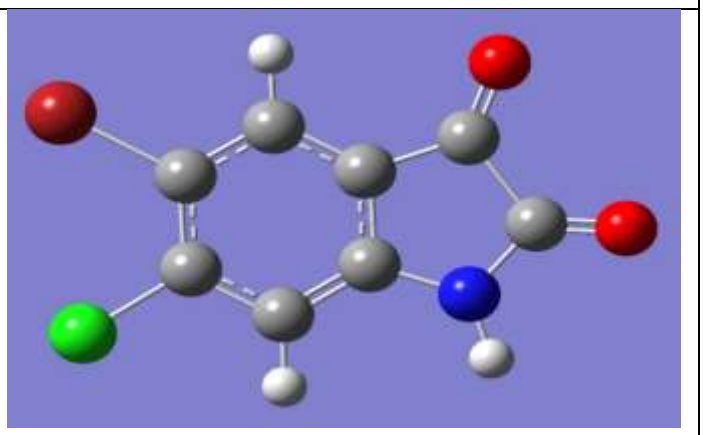
IST-10A (ENOL2)	**IST-10B (KETO)**
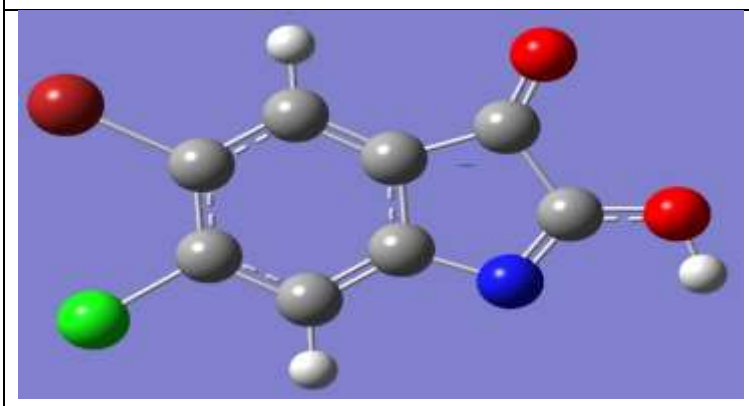	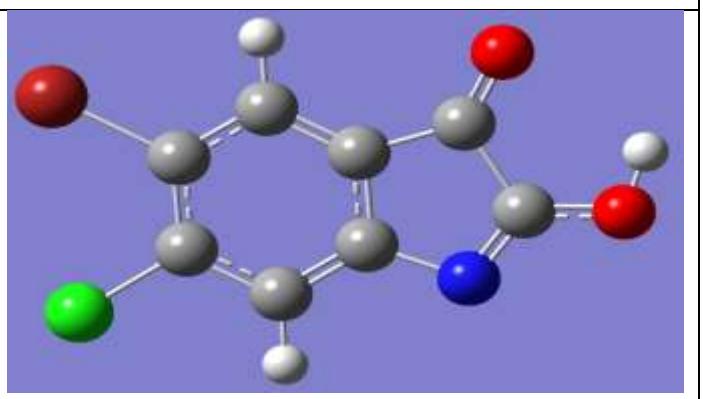
IST-10B (ENOL1)	**IST-10B (ENOL2)**
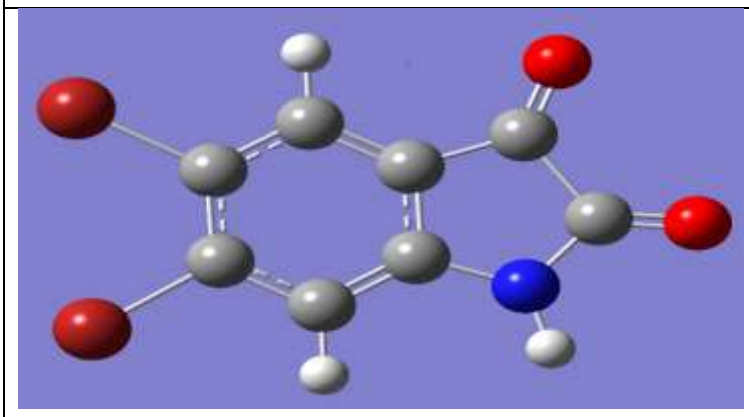	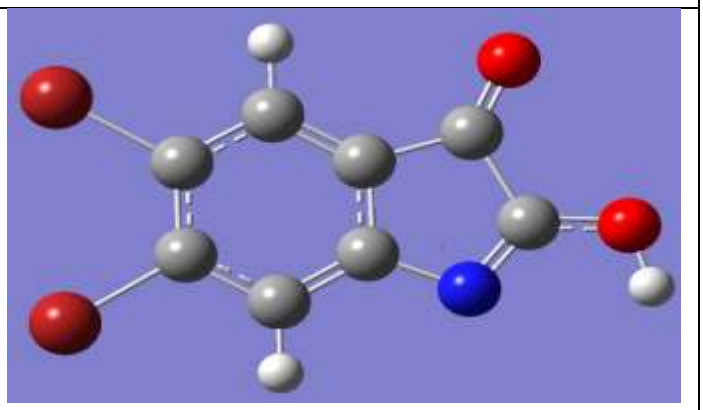
IST-10C (KETO)	**IST-10C (ENOL1)**

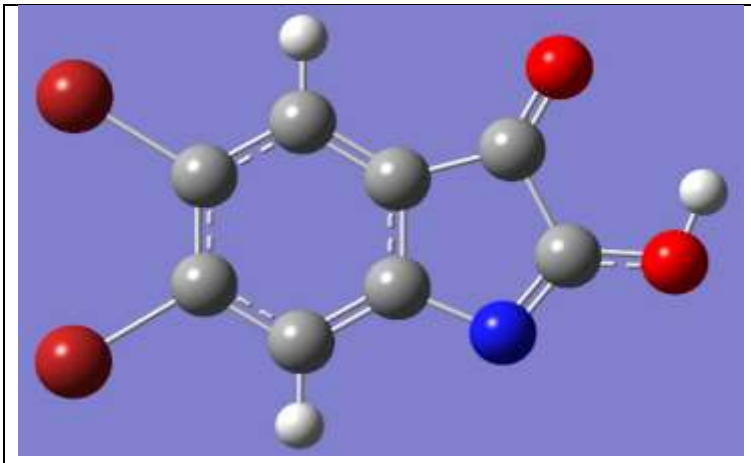	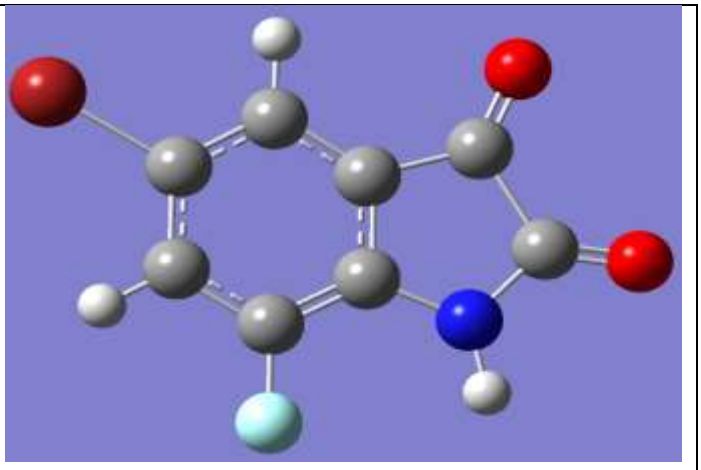
IST-10C (ENOL2)	**IST-10D (KETO)**
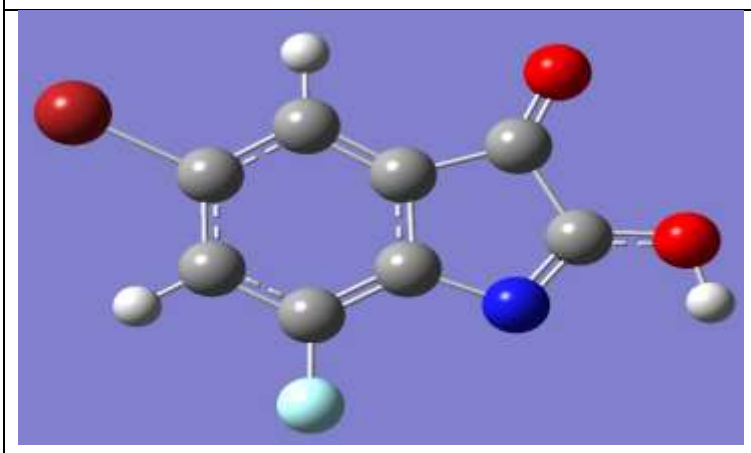	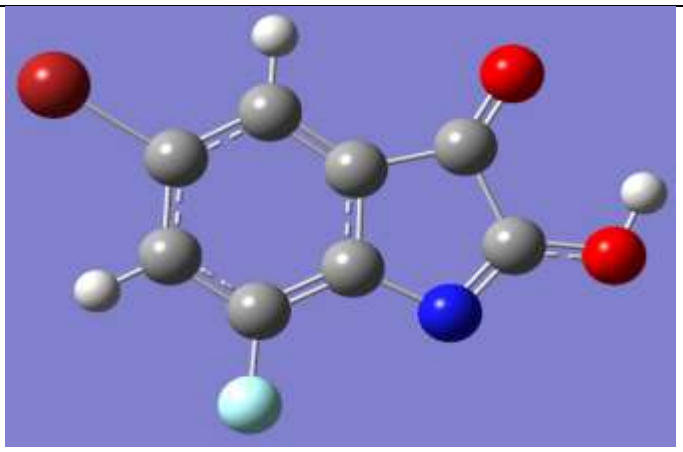
IST-10D (ENOL1)	**IST-10D (ENOL2)**
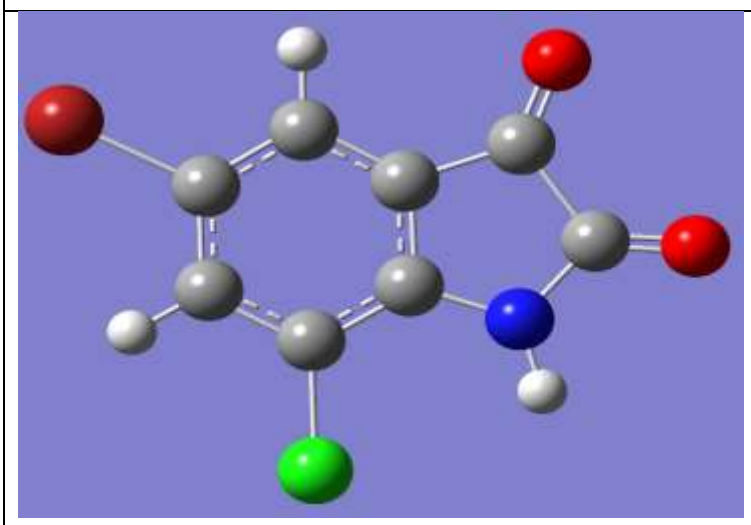	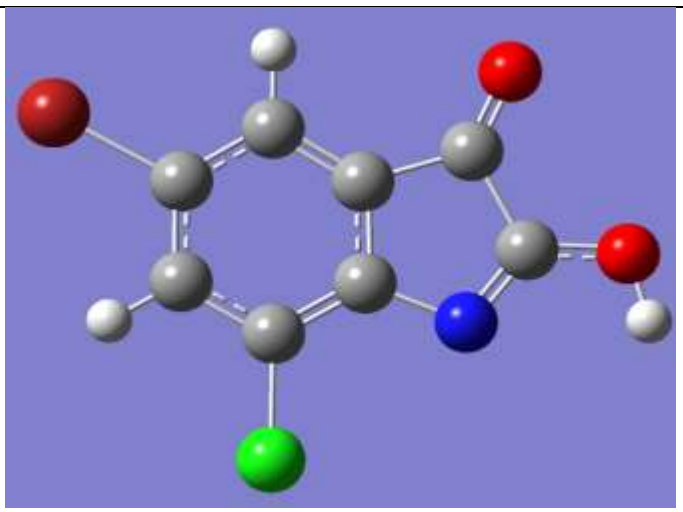
IST-10E (KETO)	**IST-10E (ENOL1)**

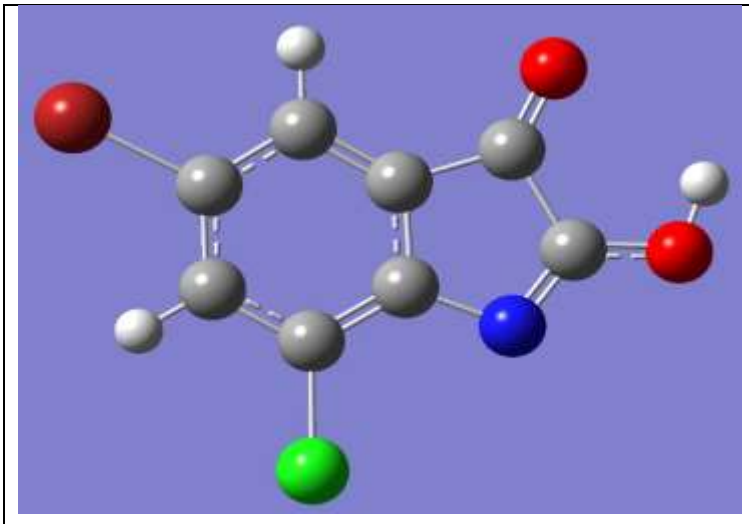

IST-10E (ENOL2)

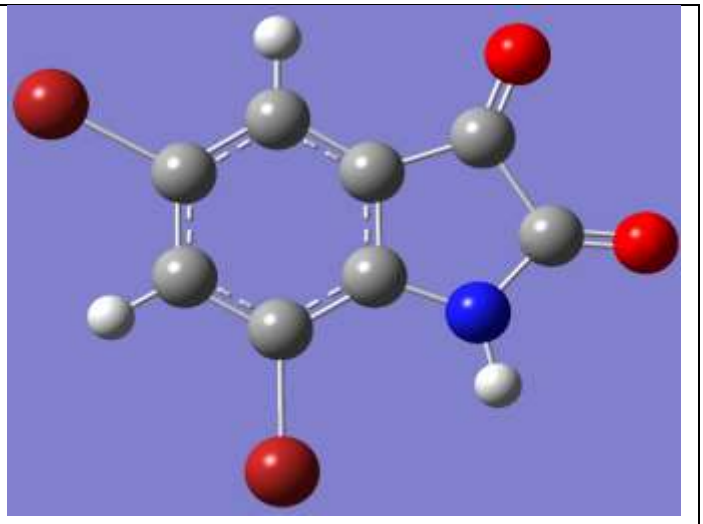

IST-10F (KETO)

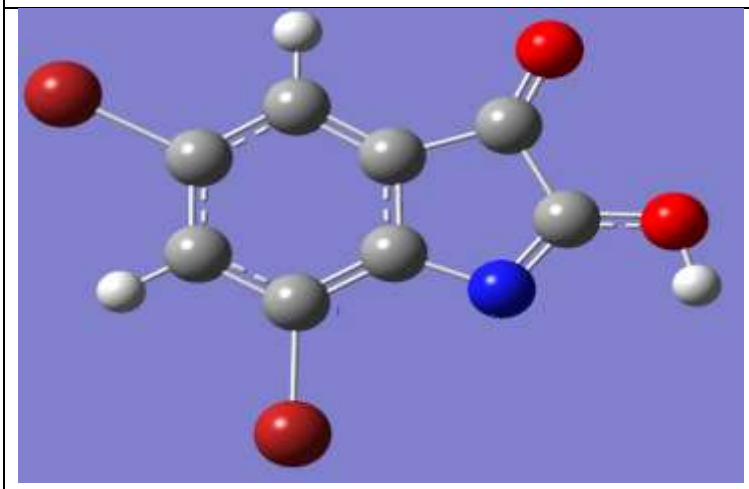

IST-10F (ENOL1)

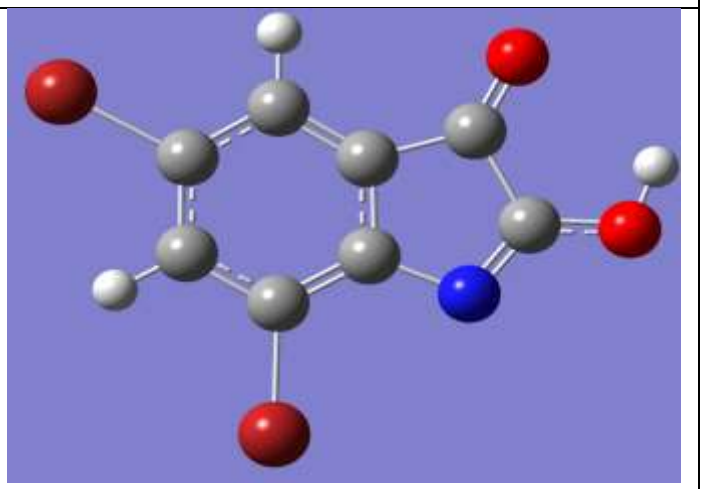

IST-10F (ENOL2)

Figure 2B3LYP/6-311G**++ geometry optimized tautomers and conformers of isatin and its halogen derivatives [Color Code: Carbon (Grey), Hydrogen (White), Oxygen (Red), Nitrogen (Blue), Fluorine (Light Blue), Chlorine (Green), Bromine (Dark Red)]

3. Results and Discussion

3.1 Relative Energies in Gas Phase

Relative energy of all low energy conformers of isatin and itsderivatives are arrangedin increasing order in Table 1, 2 and 3. From the analysis of the energy data reported in Table 1, 2 and 3 it is clear that keto conformer of isatin and all the halogen derivatives of isatin is the most stable one.Therefore, the population of keto conformer of isatin and its derivatives is maximum at room temperature and hence we confine ourselves to the discussion of keto conformer only. From the Table1 we may suggest that substitution of bromine at tenth position of isatin increases its stability. Out of all the keto conformers of 10-Bromoisatin, 10C and 10F is the most stable one suggesting that bromine present at ninth (10F) and eleventh position (10C) increases the stability of 10-Bromoisatin. Upon analysing relative energy data of 10-Bromoisatin we may conclude that the stability increases as we change halogen from F to Br at position 11^{th} and 9^{th}.

Table 1 Relative energy of keto conformer of isatin and its halogen derivatives

KETO				
SPECIES	**E (Kcal/mol)**	**ZPVE (Kcal/mol)**	**E_{tot} (Kcal/mol)**	**Relative Energy (Kcal/mol)**
ISATIN	-322042.2053	71.09717451	-321971.1081	3229851.374
4	-1936961.415	64.67278851	-1936896.742	1614925.74
4A	-1999250.639	59.5932647	-1999191.046	5551013.528
4B	-2225374.941	58.65484106	-2225316.286	1326506.196
4C	-3551878.195	58.22821392	-3551819.967	2.51579653
4D	-1999249.71	59.56826602	-1999190.142	1552632.341
4E	-2225376.831	58.71903168	-2225318.112	1326504.37
4F	-3551880.789	58.30609406	-3551822.482	0

Table 2 Relative energy of enol1 conformer of isatin and its halogen derivatives

ENOL1				
SPECIES	**E (Kcal/mol)**	**ZPVE (Kcal/mol)**	**E_{tot} (Kcal/mol)**	**Relative Energy (Kcal/mol)**
ISATIN	-322028.0987	71.07057575	-321957.0282	3229865.454
4	-1936947.73	64.65730137	-1936883.073	1614939.409
4A	-1999237.22	59.59159549	-1999177.628	1552644.854
4B	-2225361.584	58.64571471	-2225302.938	1326519.544
4C	-3551864.821	58.24586412	-3551806.575	15.90741427
4D	-1999235.549	59.5826173	-1999175.966	1552646.516
4E	-2225362.151	58.69860604	-2225303.452	1326519.03
4F	-3551866.009	58.27514942	-3551807.734	14.7482289

Table 3 Relative energy of enol2 conformer of isatin and its halogen derivatives

ENOL2				
SPECIES	**E (Kcal/mol)**	**ZPVE (Kcal/mol)**	**E_{tot} (Kcal/mol)**	**Relative Energy (Kcal/mol)**
ISATIN	-322028.2178	71.07429938	-321957.1435	3229865.339
4	-1936947.691	64.64637741	-1936883.044	1614939.438
4A	-1999237.291	59.59078558	-1999177.7	1552644.782
4B	-2225361.582	58.64066756	-2225302.941	1326519.541
4C	-3551864.818	58.21599607	-3551806.602	15.88033236
4D	-1999235.121	59.55795443	-1999175.563	1552646.919
4E	-2225361.707	58.66545883	-2225303.041	1326519.441
4F	-3551865.61	58.23756744	-3551807.373	15.10967989

3.2 NBO Analysis of Isatin (IST)

Table 4 Natural bond orbital (NBO) analysis of Isatin

S.No.	DONOR ORBITAL	OCCUPANCY	ACCEPTOR ORBITAL	OCCUPANCY	INTERACTON ENERGY (Kcal/mol)
1	π(C4-C8)	1.64662	π*(C5-C9)	0.3644	24.89
2	π(C4-C8)	1.64662	π*(C10-C11)	0.32994	16.06
3	π(C5-C9)	1.65015	π*(C4-C8)	0.36938	15.88
4	π(C5-C9)	1.65015	π*(C10-C11)	0.32994	23.11
5	π(C10-C11)	1.64738	π*(C4-C8)	0.36938	24.38
6	π(C10-C11)	1.64738	π*(C5-C9)	0.3644	16.37
7	π(O1- C6)	1.96181	π*(O2-C7)	0.2196	4.82
8	π(O1- C6)	1.96181	π*(C4-C8)	0.36938	4.58
9	π(O2- C7)	1.976	π*(O1-C6)	0.13397	4.35
10	π(C4-C8)	1.64662	π*(O1-C6)	0.13397	20.44
11	n2(O2)	1.84432	σ*(N3-C7)	0.08317	27.66
12	n2(O2)	1.84432	σ*(C6-C7)	0.14486	24.46
13	n2(O1)	1.84432	σ*(C4-C6)	0.06713	19.25
14	n2(O1)	1.86408	σ*(C6-C7)	0.14486	27.44
15	n1(N3)	1.6763	π*(O2-C7)	0.2196	50.77
16	n1(N3)	1.6763	π*(C5-C9)	0.3644	38.27
17	n1(O1)	1.98144	RY*1(C6)	0.01473	16.65
18	n1(O2)	1.98045	RY*1(C7)	0.01459	17.36
19	σ(C4-C8)	1.97494	σ*(C4-C5)	0.02865	4.77
20	σ(C5-C9)	1.97682	σ*(C4-C5)	0.02865	4.76
21	σ(C8-H13)	1.97918	σ*(C4-C5)	0.3644	4.61
22	σ(C9-C11)	1.97563	σ*(N3-C5)	0.02687	6.22
23	CR1(O1)	1.99975	RY*1(C6)	0.01473	6.67
24	CR1(O2)	1.99974	RY*1(C7)	0.01459	6.87

First six $\pi \rightarrow \pi^*$ transitions(1 to 6) indicates presence of highly conjugated benzene system. Next four transitions (7 to 10) suggests resonating system comprising C8-C4-C6-O1-C7-O2. It is to be noted that $\pi \rightarrow \pi^*$ transition of S.No. 8 is reversed of S.No. 10. Also interaction energy of latter (20.44 Kcal/mol) is higher than former (4.58 Kcal/mol) due to the stability of negative charge on electronegative oxygen. The transition atS.No. 11 and 12 indicates the transfer of electron density of lone pair of O2 to σ*(N3-C7) and σ*(C6-C7) with an interaction energy of 27.66 Kcal/mol and 24.46 Kcal/mol respectively. The transition atS.No. 13 and 14 indicates the transfer of electron density of lone pair of O1 to σ*(C4-C6) and σ*(C6-C7) with an interaction energy of 19.25 Kcal/mol and 27.44 Kcal/mol respectively. Also σ*(C6-C7) has higher occupancy than σ*(N3-C7) and σ*(C4-C6) because σ*(C6-C7) gains electron density from lone pair of O1 as well as O2. n→σ* transition from S.No. 11 to 14 can be explained by hyperconjugative effect. The transition at S.No. 15 and 16 indicates the transfer of electron density of lone pair of N3 atom to π*(O2-C7) and π*(C5-C9) with an

interaction energy of 50.77 Kcal/mol and 38.27 Kcal/mol respectively. This high interaction energy suggests the presence of powerful resonance effect pertaining to the transfer of electron density of lone pair of N3 to π* molecular orbitals.The interaction at S.No. 17 and 18 in Table 4 suggests that electron density from non bonding orbital of O1 and O2 is transferred to an antibonding Rydberg orbital associated with C6 and C7 with an interaction energy of 16.65 Kcal/mol and 17.36 Kcal/mol respectively which results in decrease in electron density on O1.σ(C4-C8) to σ*(C4-C5) and σ(C5-C9) to σ*(C4-C5) interactions suggest that electrons in the σ bonds between C4-C8 and C5-C9 are delocalized into σ* orbital of C4-C5. This delocalization helps to stabilize the molecule by spreading electron density over a larger volume and reducing electron electron repulsions within the molecule. σ(C8-H13) to σ*(C4-C5) and σ(C9-C11) to σ*(N3-C5) interaction represents hyperconjugation effect where electron density from C-H and C-C σ bond is delocalized into nearby σ* orbital contributing to overall stability. The interaction at S.No. 23 and 24 in Table 4 describe the process wherein electron density is transferred between deeply bound core electrons of O1 and O2 to diffuse antibonding Rydberg orbitals associated with C6 and C7.

3.3 Comparison of NBO analysis of derivatives of Isatin (IST)

Table 5 Interaction energies of donor and acceptor orbitals in Kcal/mol for Isatin and its halogen derivatives

S.No.	DONOR ORBITAL	ACCEPTOR ORBITAL	IST	IST-10	IST-10A	IST-10B	IST-10C	IST-10D	IST-10E	IST-10F
1	π(C4-C8)	π*(O1-C6)	20.44	19.69	20.34	19.87	19.73	18.72	18.9	18.91
2	π(C4-C8)	π*(C5-C9)	24.89	24.17	25.55	24.54	24.37	23.1	24.95	24.94
3	π(C4-C8)	π*(C10-C11)	16.06	16.84	15.78	17.34	17.34	18.15	17.38	17.26
4	π(C10-C11)	π*(C5-C9)	16.37	14.79	13.34	13.88	14.1	17.11	15.12	14.95
5	π(C10-C11)	π*(C4-C8)	24.38	23.28	23.95	21.39	21.03	21.23	22.22	22.43
6	π(C5-C9)	π*(C4-C8)	15.88	16.58	14.64	15.53	15.77	17.13	14.99	14.76
7	π(C5-C9)	π*(C10-C11)	23.11	24.74	27.12	24.47	24.28	23.03	23.25	23.47
8	π*(C10-C11)	π*(C4-C8)	-	204.05	111.76	96.51	99.04	167.38	174.14	174.44
9	π*(C10-C11)	π*(C5-C9)	-	-	184.62	114.69	117.13	-	-	-
10	π*(C5-C9)	π*(C4-C8)	-	-	283.66	-	-	191.27	156.24	162.69
11	CR1(O1)	RY*1(C6)	6.67	6.7	6.68	6.68	6.68	6.72	6.7	6.7
12	CR1(O2)	RY*1(C7)	6.87	6.88	6.89	6.89	6.88	6.88	6.86	6.85
13	n1(O1)	RY*1(C6)	16.65	16.66	16.62	16.63	16.59	16.75	16.67	16.65
14	n1(O2)	RY*1(C7)	17.36	17.37	17.75	17.75	17.73	17.63	17.63	17.62
15	n1(X16)	RY*1(C11)	-	-	8.47	1.96	1.02	-	-	-
16	n1(X16)	RY*1(C9)	-	-	-	-	-	7.44	1.86	1.23
17	n1(N3)	π*(O2-C7)	50.77	50.33	49.1	48.53	49.61	49.66	49.48	49.61
18	n1(N3)	π*(C5-C9)	38.27	38.53	40.8	39.71	39.46	39.75	43.04	43.21
19	n3(Br15)	π*(C10-C11)	-	9.46	10.31	11.02	10.99	10.03	9.85	9.81
20	n3(X16)	π*(C10-C11)	-	-	21.52	15.72	12.47	-	-	-
21	n3(X16)	π*(C5-C9)	-	-	-	-	-	16.93	11.99	9.5
22	n2(O1)	σ*(C4-C6)	19.25	19.61	19.62	19.75	19.77	19.96	19.98	20
23	n2(O1)	σ*(C6-C7)	27.44	27.56	27.74	27.64	27.59	27.55	27.51	27.47
24	n2(O2)	σ*(N3-C7)	27.66	27.81	28.25	28.2	28.14	28.24	28.23	28.17
25	n2(O2)	σ*(C6-C7)	24.46	24.71	24.63	24.72	28.64	24.93	24.88	24.85

26	n2(X16)	σ*(C9-C11)	-	-	6.16	4.08	3.14	6.25	4.42	3.48
27	n2(X16)	σ*(C10-C11)	-	-	6.08	4.46	3.65	-	-	-
28	n2(X16)	σ*(C5-C9)	-	-	-	0.51	-	6.08	4.4	3.5

Upon comparing various transitions among all eight species through NBO analysis, it has been found that $\pi^* \rightarrow \pi^*$ and n $\rightarrow$ RY* transitions are not observed for isatin. The difference in the interaction energy values for $\pi^* \rightarrow \pi^*$ transition is significant. It has been observed that halogen at 11th position reduces interaction energy more than at 9th position for π^* (C10-C11) $\rightarrow \pi^*$ (C4-C8) transition. In case of dihalogen derivatives of isatin, highest interaction energy for transition at S.No.8 is observed for IST-10E and IST-10F. Also, interaction energy for transition π^* (C10-C11) $\rightarrow \pi^*$ (C5-C9) molecular orbital is maximum for IST-10A and the same is not observed for IST, IST-10, 10D, 10E and 10F. Additionally interaction energy for transfer of electron density from π^* (C5-C9) to π^* (C4-C8) is maximum for Bromofluoro derivatives and this interaction is not observed in IST, IST-10, IST-10B and 10C. Interaction energy corresponding to the transfer of electron density from CR(O1), CR(O2), n1(O1) and n1(O2) to RY*1(C6) and RY*1(C7) do not show much variation among all species. Interaction energy from n1(X16) $\rightarrow$ RY* (C11/C9) is maximum for Fluorobromo derivative of isatin. Chlorobromo and dibromo derivatives share almost similar interaction energy for the same transition.For the electron transfer from n1(N3) to π*(O2-C7), the energy values decrease from IST to IST-10B, then slightly increase towards IST-10F. The highest energy is at IST (50.77), and the lowest is at IST-10B (48.53) indicating that mono halo and di halo derivatives of isatin show less +R effect as compared to core isatin involving lone pair of N3 to π orbital of O2—C7 bond. For π*(O2-C7), there is a decrease in energy up to IST-10B, which may suggest a less favorable or less efficient electron transfer. IST-10C and IST-10F have same value of interaction energy (49.61 Kcal/mol) for transfer of electron density to π*(O2-C7) indicating that position of -Br either at 9th or 11this not affecting the interaction. Also On the other hand, the energy required for electron transfer to π*(C5-C9) becomes higher in the later species (IST-10C to IST-10F), indicating more favorable conditions for electron transfer. For the electron transfer from n1(N3) to π*(C5-C9), jump in the interaction energy is observed from IST-10 to IST-10A and from IST-10D to IST-10E. IST-10E and IST-10F share almost same interaction energy for electron transfer from n1(N3) to π*(C5-C9). The lowest interaction energy is at IST (38.27), and the highest is at IST-10F (43.21 Kcal/mol). The interaction energy at S.No.19 is max for IST-10B and IST 10C and minimum for IST-10F. Bromine present at 10th position is able to give electrons through +R effect to π*(C10-C11) provided halogen is present at 11th position rather than 9th position. Also this +R effect is maximum for chlorine and bromine present at 11th position. Out of the three halogens viz. F, Cl and Br present at position 11th and 9thfluorine transfers electron density to π*(C10-C11) and π*(C5-C9) with maximum interaction energy of 21.52 Kcal/mol and 16.93 Kcal/mol respectively due to better overlap of 2p orbitals of carbon and fluorine. The hyperconjugative effect which explains the transfer of electron density from lone pair of O1 to σ*(C4-C6) and σ*(C6-C7) is maximum for Dibromo and Bromofluoro derivatives of isatin respectively. The maximum hyperconjugative effect corresponding to the transfer of electron density of lone pair of O2 to σ*(N3-C7) and σ*(C6-C7) is observed

for IST-10A (28.25) and IST-10D (28.93) respectively indicating that Fluorobromoderivatives of isatin are more efficient in this electron transfer. The hyperconjugation effect involving the transfer of electron density from lone pair of halogen situated at 11^{th} or 9^{th} position to σ*(C9-C11), σ*(C10-C11) and σ*(C5-C9) is maximum for Flurorobromo derivatives of isatin and minimum for dibromoderivatives of isatin.

3.3 NMR Spectra

The NMR spectra were calculated at the B3LYP/6-311++G** level in DMSO solvent by using the gauge-independent atomic orbital method [26] that provides magnetic shielding constants. The chemical shifts for carbon and hydrogen atoms were obtained on the δ-scale relative to TMS through the equation,

$\delta_i = \sigma^{TMS} - \sigma_i$

where the values of σ^{TMS} (31.96 for H and 185.0 for C) were obtained at the same level of calculation (B3LYP/6-311++G**). Theoretically calculated chemical shifts for ^{13}C and ^{1}H are listed in Table 6.

Table 6 Calculated natural charge and chemical shifts (ppm) of carbons and hydrogens

	IST		IST-10		IST-10A		IST-10B	
Atom	**Shift**	**Charge**	**Shift**	**Charge**	**Shift**	**Charge**	**Shift**	**Charge**
C4	124.564	-0.2079	125.298	-0.18762	121.2706	-0.19911	123.3112	-0.18849
C5	159.9361	0.2191	158.128	0.22066	160.218	0.23769	158.4222	0.22697
C6	193.9501	0.49613	193.564	0.4997	190.9358	0.49693	191.7496	0.49797
C7	166.745	0.6245	166.324	0.62538	166.3144	0.62821	165.9358	0.62612
C8	134.2454	-0.1187	136.936	-0.1439	140.2008	-0.12345	138.8256	-0.12423
C9	118.9857	-0.243	120.847	-0.22184	108.7619	-0.28064	121.993	-0.22883
C10	130.9688	-0.2334	142.298	-0.13473	128.2236	-0.19881	141.5176	-0.16556
C11	149.0517	-0.1313	151.068	-0.15596	177.4557	0.44677	162.4994	-0.02605
H12	7.0995	0.43063	7.2173	0.43329	7.2372	0.43534	7.2024	0.43444
H13	7.8687	0.22844	7.8877	0.24312	7.9735	0.24665	7.9606	0.24686
H14	7.0613	0.23304	7.0589	0.2394	6.9156	0.25473	7.2245	0.2496
H15	7.3026	0.22266	-	-	-	-	-	-
H16	7.8401	0.22153	7.7783	0.23641	-	-	-	-

	IST-10C		IST-10D		IST-10E		IST-10F	
Atom	**Shift**	**Charge**	**Shift**	**Charge**	**Shift**	**Charge**	**Shift**	**Charge**
C4	124.2196	-0.18729	126.6333	-0.16636	126.3523	-0.16721	126.4627	-0.16721
C5	157.4682	0.23285	144.6077	0.15689	155.1738	0.19061	156.5134	0.19061
C6	192.1113	0.49808	192.2966	0.50118	192.9354	0.50178	191.9173	0.50178
C7	165.9747	0.62573	165.2086	0.62568	165.2632	0.62744	164.5458	0.62744
C8	138.3977	-0.12312	133.3909	-0.15494	135.6852	-0.1441	135.8127	-0.1441
C9	124.5441	-0.24413	156.3723	0.39281	132.637	-0.06356	131.0954	-0.06356
C10	144.3695	-0.16978	142.3351	-0.12197	142.5798	-0.12181	142.2025	-0.12181
C11	164.6311	-0.08869	137.7904	-0.22052	150.1429	-0.18044	152.549	-0.18044
H12	7.1438	0.43446	7.3241	0.43962	7.4102	0.43911	7.2659	0.43911
H13	7.8894	0.24685	7.7304	0.24677	7.7594	0.24694	7.69	0.24694

H14	7.2719	0.24952	7.6236	0.25287	7.8113	0.24944	7.9239	0.24944
H15	-	-	-	-	-	-	-	-
H16	-	-	-	-	-	-	-	-

The chemical shift varies with the charge on the atom. Therefore, we performed regression analysis of the theoretically calculated chemical shift with respect to the natural charge densities (Table 6) for the C atoms and H atoms of derivatives of isatin. The polynomial fit of the two variables yielded the following equations for the halogen substituted isatin along with regression coefficient.

3.3.1 Equations for Carbon shift v's Charge

$\delta_{IST} = 482355q^6 – 372447q^5 – 50759q^4 + 56229q^3 + 5410.3q^2 – 1759.9q – 53.93$ ($r^2 = 0.965$)

$\delta_{IST\text{-}10} = 10^6q^6 – 10^6q^5 – 101683q^4 + 162553q^3 + 12527q^2 – 5043.5q – 397.83$ ($r^2 = 0.9745$)

$\delta_{IST\text{-}10A} = -15765q^6 + 7565.7q^5 + 4400.4q^4 – 1161.6q^3 – 628.64q^2 – 131.61q + 163.11$ ($r^2 = 0.996$)

$\delta_{IST\text{-}10B} = -28619q^6 + 18323q^5 + 4646.7q^4 - 2380q^3 – 680.32q^2 + 155.29q – 166.62$ ($r^2 = 0.9725$)

$\delta_{IST\text{-}10C} = -180170q^6 – 138215q^5 + 18486q^4 - 20366q^3 – 2121.4q^2 + 760.78q + 232.23$ ($r^2 = 0.9394$)

$\delta_{IST\text{-}10D} = 35067q^6 – 60717q^5 + 26722q^4 + 1922.5q^3 – 2248.3q^2 + 33.959q + 176.24$ ($r^2 = 0.9972$)

$\delta_{IST\text{-}10E} = 2X10^6q^6 – 10^6q^5 + 123280q^4 + 129849q^3 – 1715.5q^2 – 2812.9q – 9.7467$ ($r^2 = 0.985$)

$\delta_{IST\text{-}10F} = 2X10^6q^6 – 2X10^6q^5 + 130874q^4 + 137072q^3 – 1767q^2 – 2969.1q – 19.391$ ($r^2 = 0.9816$)

3.3.2 Equations for Hydrogen shift v's Charge

$\delta_{IST} = 5X10^7q^4 – 5X10^7q^3 + 2X10^7q^2 - 4X10^6q + 232221$ ($r^2 = 1.0006$)

$\delta_{IST\text{-}10} = -35670q^3 + 325506q^2 - 94552q + 8881.4$ ($r^2 = 1$)

$\delta_{IST\text{-}10A} = 703.32q^2 – 483.56q + 84.456$ ($r^2 = 1$)

$\delta_{IST\text{-}10B} = 1431.5q^2 – 979.36q + 162.49$ ($r^2 = 1$)

$\delta_{IST\text{-}10C} = 1229q^2 – 841.33q + 140.68$ ($r^2 = 1$)

$\delta_{IST\text{-}10D} = 82.471q^2 – 98.714q + 17.197$ ($r^2 = 1$)

$\delta_{IST\text{-}10E} = -119.03q^2 + 79.846q – 4.6992$ ($r^2 = 1$)

$\delta_{IST\text{-}10F} = -504.91q^2 + 344.19q – 46.515$ ($r^2 = 1$)

The agreement between the calculated carbon chemical shift values with natural charge varies between 93.94 % to 99.72 % for all the eight species viz. IST, IST-10, IST-10A, IST-10B, IST-10C, IST-10D, IST-

10E and IST-10F. Also, the agreement between calculated hydrogen shift values with natural charge is 100 % for all the eight species.

3.4 UV vis Spectra

The calculated UV-Vis spectrum for various isatin and halogen substituted isatin using the TD-DFT method in DMSO solvent across three electronic states (ES1, ES2, ES3) are given in Table 7. For each state, the data includes orbital transition (orbital number), energy of transition in electron volts (eV), wavelength of light absorbed (λ in nm) and oscillator strength (f), which is a measure of the probability of the transition. The electronic states represent low energy low efficiency transitions in ES1 through slightly higher energy transitions in ES2 to high energy high efficiency transitions in ES3. ES1 involves the lowest energy transitions with absorption in visible spectrum characterized by longer wavelength. The energy transitions in ES2 are slightly higher than ES1 moving the absorption into shorter wavelengths within the visible range. ES3 represents the highest energy state with absorption in UV range. The oscillator strength values in ES1 are generally low with many compounds showing f-values of zero indicating forbidden transitions in this state. The oscillator strength in ES3 are notably higher, indicating stronger and more probable transitions. Compounds IST-10B and IST-10C show high f-values in ES3 suggesting that they have strong absorption in this state. From Table 7, it is observed that oscillator strength is maximum in case of ES3, therefore we may call, its wavelength to be λ_{max} i.e. corresponding to maximum oscillator strength. Upon analysing the data of ES3, we may say that λ_{max}decreases on introducing -Br at 10^{th} position of Isatin. Introduction of halogen either at 9^{th} or 11^{th} position of 10-Bromoisatin increases $\lambda_{max}$and this incrementis more pronounced for 9^{th} position. Also, as electronegativity of halogen decreases, λ_{max} increases. This may be explained on the basis of increase in +R effect with decreased electronegativity of halogen. It has been observed from Table 7that ‘f’ has higher value for isatin as compared to its derivatives except for IST-10B and IST-10C. Among the derivatives, as electronegativity of halogen decreases, value of ‘f’ increases if halogen is placed at 11^{th} position and decreases if halogen is placed at 9^{th} position, with maximum being found for IST-10B and IST-10C.

Table 7 UV-vis Spectra for IST and its halogen derivatives

	ES1				ES2			
SPECIES	**ORBITAL NO**	**ENERGY (ev)**	**λ (nm)**	**f**	**ORBITAL NO**	**ENERGY IN ev**	**λ (nm)**	**f**
IST	37 to 39	2.8194	439.75	0	38 TO 39	2.8789	430.67	0.0253
IST-10	55 TO 56	2.7137	456.87	0.0247	54 TO 56	2.7892	444.52	0
IST-10A	58 TO 60	2.8288	438.29	0	59 TO 60	2.8355	437.26	0.0225
IST-10B	63 TO 64	2.7794	446.09	0.0276	62 TO 64	2.7891	444.53	0
IST-10C	72 TO 73	2.7666	448.15	0.0288	71 TO 73	2.7816	445.73	0
IST-10D	59 TO 60	2.7044	458.45	0.0319	58 TO 60	2.7735	447.03	0
IST-10E	63 TO 64	2.6883	461.2	0.0318	62 TO 64	2.774	446.94	0
IST-10F	72 TO 73	2.6449	468.77	0.0308	71 TO 73	2.791	444.23	0

	ES3			
SPECIES	ORBITAL NO	ENERGY IN ev	λ (nm)	f
IST	36 TO 39 AND 38 TO 40	4.1377	299.65	0.1487
IST-10	51 TO 56 AND 53 TO 56 AND 55 TO 57	4.2124	294.33	0.1078
IST-10A	57 TO 60 AND 59 TO 61	4.1873	296.09	0.1209
IST-10B	61 TO 64 AND 63 TO 65	4.0033	309.7	0.2298
IST-10C	70 TO 73 AND 72 TO 75	3.8655	320.75	0.2768
IST-10D	57 TO 60 AND 59 TO 61	4.1005	302.36	0.1318
IST-10E	61 TO 64 AND 63 TO 65	3.9275	315.68	0.093
IST-10F	70 TO 73 AND 72 TO 74	3.7796	328.04	0.067

3.5 Thermochemistry

The data in Table 8 shows values of ΔH° and ΔG° for keto-enol tautomerism and conformational isomerisation for enol form of isatin and its various derivatives.

Table 8 ΔH° and ΔG° values in Kcal/mol for Tautomerisation and Conformational isomerisation

SPECIES	ΔH°_{tauto}	ΔH°_{iso}	ΔG°_{tauto}	ΔG°_{iso}
IST	14.032984	-0.123	14.1917	-0.08848
IST-10	13.621338	0.02698	13.782	0.048318
IST-10A	13.362804	-0.0772	13.531	-0.05083
IST-10B	13.300681	-0.0088	13.4557	0.018198
IST-10C	13.333939	-0.0257	13.5165	-0.01004
IST-10D	14.11958	0.40474	14.2878	0.420431
IST-10E	14.616567	0.41353	14.7509	0.431099
IST-10F	14.711949	0.36898	14.8337	0.36772

3.5.1 Keto-Enol Tautomerisation

The values of ΔH° and ΔG° are quite close for each species, suggesting effect of temperature on ΔG° is not dominant or change in entropy (ΔS°) is relatively small. As we move from species IST-10 to IST-10F there is a general trend of increasing ΔH° and ΔG°, suggesting that the later species (IST-10E and IST-10F) have reactions that are increasingly endothermic and less spontaneous compared to earlier ones (IST-10, IST-10A, IST-10B etc.). Isatin and IST-10D are sharing similar ΔH° and ΔG° values indicating similar energetic profile for keto-enol tautomerism and conformational isomerisation. Species IST-10E and IST-10F show highest values, suggesting they are the most energetically demanding to form. Therefore, we can conclude that introducing halogen at 9^{th} position is less favourable thermodynamically than at 11^{th} position. Nature of halogen present at 11^{th} position does not affect much the values of ΔH° and ΔG° whereas at 9^{th} position it affects ΔH° and ΔG° significantly. The species having halogen present at 11^{th} position is thermodynamically easy to form than at 9^{th} position as indicated by their ΔG° values.

3.5.2 Conformational Isomerisation of Enol Form

It is clear from the data reported in Table 8 that ΔH° and ΔG° for the conformational isomerisation of Enol is approximately zero for all the species which suggests that there is no significant heat exchange with the surroundings during the process, indicating it is neither strongly exothermic nor endothermic and also the process is very close to equilibrium implying no significant spontaneous reaction in either direction under standard conditions.

3.6 Global Reactivity Parameters

Table 9 Global reactivity parameters of isatin and its halogen derivatives

SPECIES	HOMO (ha)	LUMO (ha)	HOMO NO	LUMO NO	HLG (ha)	DM (Debye)
IST	-0.25576	-0.04231	38	39	0.21345	6.3848
IST-10	-0.25491	-0.12341	55	56	0.1315	5.6031
IST-10A	-0.26107	-0.12524	59	60	0.13583	4.2493
IST-10B	-0.26057	-0.12751	63	64	0.13306	4.4989
IST-10C	-0.26014	-0.1277	72	73	0.13244	4.6334
IST-10D	-0.26137	-0.13067	59	60	0.1307	4.3143
IST-10E	-0.26094	-0.13082	63	64	0.13012	4.4052
IST-10F	-0.26038	-0.13061	72	73	0.12977	4.5247

χ (ha)	μ (ha)	η (ha)	S (ha)	ω (ha)	N (ha)
-0.149035	0.149035	0.106725	4.6849379	0.0745175	0.09291
-0.18916	0.18916	0.06575	7.6045627	0.09458	0.09376
-0.193155	0.193155	0.067915	7.3621439	0.0965775	0.0876
-0.19404	0.19404	0.06653	7.5154066	0.09702	0.0881
-0.19392	0.19392	0.06622	7.5505889	0.09696	0.08853
-0.19602	0.19602	0.06535	7.6511094	0.09801	0.0873
-0.19588	0.19588	0.06506	7.6852136	0.09794	0.08773
-0.195495	0.195495	0.064885	7.7059413	0.0977475	0.08829

*Figures in parenthesis are HOMO No. and LUMO No.

To understand electronic properties and potential chemical reactivity of isatin and its derivatives we calculated various Global Reactivity Parameters from HOMO LUMO values of the molecules.

3.6.1 HLG (HOMO LUMO Gap)

Starting from isatin and moving towards the derivatives labelled IST-10 through IST-10F, there is a general trend of narrowing HLG. This trend suggests that introduction of X at any position (10^{th}/11^{th}/9^{th}) alters the electronic properties of molecules in such a way that HLG decreases. Introduction of -Br at 10^{th} position of isatin decreases its HLG significantly and hence increases the electron mobility within molecule. Among the derivatives HLG decreases from IST-10A to IST-10F with the smallest gaps observed for IST-10E and IST-10F, indicating that 9^{th} position decreases HLG more than at 11^{th} position of 10-Bromoisatin. This may be attributed to the less steric hinderance at position 9^{th} than 11^{th}, due to which lone pair of halogen at 9^{th} position can enter into resonance better than 11^{th} position.

3.6.2 Dipole Moment (DM)

Although there is variability in dipole moment among all eight species, the derivatives generally have lower dipole moment as compared to isatin indicating that introduction of halogen tend to reduce molecular polarity in the isatin due to +R effect. The dipole moment decreases significantly from isatin (6.3848 D) to its first derivative IST-10 (5.6031 D) suggesting a reduction in molecular polarity, which indicates that introduction of Br at position 10^{th} of isatin ring makes charge distribution more symmetrical, due to its -I effect. Among the derivatives, there is a range of dipole moment values from as low as 4.2493 D (IST-10A) to as high as 4.6334 D (IST-10C). It has been observed from dipole moment values that fluoro derivative of IST-10 at 11^{th} position has less dipole moment than at 9^{th} position suggesting that -I effect of F is more effective from 11^{th} position than 9^{th} position. The opposite is true incase of chloro and bromo derivatives of IST-10. This may be due to the large size of Cl and Br which results in crowding at 11^{th} position and hence its -Ieffect.

3.6.3 Electronegativity (χ)

Isatin has a χ value of -0.149035. This is the least negative value in the list suggesting that among the listed species in Table 9,Isatin has the lowest tendency to attract electrons under the conditions. Species IST-10 through IST-10F show a range of χ values from -0.18916 to -0.19602. All these values are more negative than that of isatin, indicating a higher tendency to attract electrons. This suggests that these species are more electronegative than isatin according to these χ values. The progression from IST-10A to IST-10C shows a general trend of increasing electronegativity while progression from IST-10D to IST-10F shows decreasing electronegativity with a maximum found at IST-10D. Species IST-10D has highest electronegativity (-0.19602), closely followed by species IST-10E and IST-105F. It is clear from the Table 9 that putting halogen at 9^{th} position increases electronegativity of 10-Bromoisatin more than putting halogen at 11^{th} position. Upon comparing electronegativity of IST-10A and IST-10D, we can say that -F at 9^{th} position of 10-Bromoisatin is more effective in increasing electronegativity of molecule than at 11^{th} position. So, IST-10D has greater ability to stabilize negative charge in reaction intermediates among all species.

3.6.4 Chemical potential (μ)

Isatin has μ value of 0.149035. This value serves as the baseline for comparison with other species listed in Table 9. Species IST-10to IST-10F show μ values ranging from 0.18916 to 0.19602. All these values are higher than isatin suggesting attachment of halogen increases the chemical potential of isatin. Higher chemical potential of halogenated isatins imply that they are more likely to react or participate in chemical processes as compared to isatin. Also IST-10D has highest value of μ suggesting its highest tendency to undergo reaction among all eight species. The differences among μ values of species IST-10A through IST-10F are relatively small, indicating their μ are quiet similar. From the Table 9 it is clear that halogen at 9^{th} position results in more μ than at 11^{th} position in case of 10-Bromoisatin indicating that 9^{th} position is more sensitive for hardness. IST-10D is showing maximum μ because of small size and high electronegativity of F coupled with sensitivity of 9^{th} position of 10-Bromoisatin.

3.6.5 Global hardness (η)

Isatin with η value of 0.106725, stands out as having a significantly higher global hardness compared to the other species listed in Table 9. This suggests that isatinis comparatively more resistant to change or deformation than the other species because higher hardness implies a more stable electron cloud, which is less amenable to change. The introduction of -Br at 10^{th} position of isatin decreases η value and making it more susceptible for deformation. There appears to be general trend of decreasing η from IST-10A to IST-10F suggesting that as electronegativity of halogen decreases η also decreases and change in nature of halogen at 9^{th} position of 10-Bromoisatin results in much lower value of η than 11^{th}position. Lowest value of η is reported

for IST-10F indicating that it can more easily undergo changes in electron cloud, making it more flexible to participate in chemical reactions due to low electronegativity and bigger size of -Br.

3.6.6 Global Softness (S)

Isatin with a S value of 4.684937925, has lowest softness index suggesting it to be lessreactive than others. Introduction of -Br in isatin at 10^{th} position increases its softness andhence reactivity. There seems to be a trend of increasing softness from compound IST-10A to IST-10F suggesting an increased reactivity and tendency to form chemical bonds and participate in reactions. Also as electronegativity of halogen decreases, softness increases and higher value of softness arise from halogen at 9^{th}position of 10-Bromoisatin than 11^{th} position. Highest value of S for IST-10F further confirms its highest reactivity among all eight species.

3.6.7 Global Electrophilicity Index (ƆC)

Global electrophilicity index is a quantitative measure of molecule's electrophilicity or probability to accept electrons. From Table 9, it is clear that isatin has the lowestelectrophilicity among all eight species. The introduction of halogen in isatin increasesits electrophilicity due to their -I effect. Halogen derivatives of isatin show a gradual increase in electrophilicity from IST-10 to IST-10F with IST-10E and IST-10F having nearly the same values, suggesting that they are among the strongest electrophiles in this list. The trend in electrophilicity values indicate that electron withdrawing groups enhance theelectrophilicity of isatin core.

3.6.8 Global Nucleophilicity Index (N)

N can be calculated using the following empirical equation:

$N = HOMO_{compound} - HOMO_{TCN}$

HOMO of TCN = -0.34867 ha

IST-10 has a slightly higher Global Nucleophilicity Index of 0.09376 compared to the reference IST, suggesting that it's slightly more nucleophilic. IST-10A to IST-10F are variants of what might be the original IST-10 species. Their Global Nucleophilicity Index values vary from 0.0873 to 0.08853. All of these values are lower than the reference IST and the IST-10, indicating that these variants are less nucleophilic compared to the reference.It has been observed from the data that the halogen at 11^{th} position makes 10-Bromoisatin more nucleophilic than at 9^{th} position. Also nucleophilicity of the halogen derivative of 10-Bromoisatin increases as we change the nature of halogen from F to Br due to decrease in -I effect of halogen.

3.7 Vibrational Spectra of isatin and its halogen derivatives

The calculated vibrational wavenumbers, corresponding intensities and description of isatin and its halogen derivatives are reported in Table 10-17.

Table 10 Vibrational spectra of IST

S.NO	FREQ	INTENSITY	DESCRIPTION
1	1811.13	423.023	Stretching mode of O1-C6 and O2-C7
2	1656.62	337.643	Stretching mode of C5-C9 coupled with antisymmetric stretch of C10-C8-C4 and bending mode of N3-C12, C9-H14, C110-H15, C8-H13
3	1831.85	301.833	Stretching mode of C7-O2 an C6-O1 coupled with N3-H12
4	511	115.886	Bending mode of C7-N3-H12 (wagging)
5	1496.85	84.7215	Stretching mode of C8-C10 and C4-C5 coupled with bending mode of C8-H13, C11-H16 and C9-H14
6	1348.6	64.0745	Antisymmetric stretch of C8-C4-C5, C11-C9-C5, C10-C11-C9 coupled with bending mode of C8-H13, C10-H15, C9-H14 and N3-H12
7	765.96	60.0498	Bending mode of C9-H14, C11-H16, C10-H15 and C8-H13
8	1158.15	59.2629	Antisymmetric stretch of C5-N3-C7 coupled with stretching mode of C4-C6 and N3-C7 along with bending mode of C8-H13, C10-H15, C11-H16, C9-H14 and N3-H12
9	3629.38	51.7689	Stretching mode of N3-H12
10	1190.08	51.3052	Stretching mode of C7-N3 coupled with bending mode of H15-C10, H16-C11,H14-C9 (in plane)
11	1404.7	49.0802	Antisymmetric stretch of C4-C8-C10, C8-C10-C11, C10-C11-C9 coupled with stretching mode of N3-C5 and bending mode of N3-H12, C9-H14, C11-H16, C8-H13 bonds

Table 11 Vibrational spectra of IST-10

S.NO	FREQ	INTENSITY	DESCRIPTION
1	1815.06	470.322	Stretching mode of C6-O1(major) and C7-O2(minor)
2	1834.1	295.573	Stretching mode of C6-O1(minor) and C7-O2(major) coupled with bending mode of N3-H12
3	1650.08	265.644	Antisymmetric stretch of C11-C9-C5 and C4-C8-C10 coupled with bending mode of C8-H13, C9-H14 and N3-H12 bonds
4	1491.24	154.911	Stretching mode of C4-C5 coupled with antisymmetric stretch of C8-C10-C11 and bending mode of C11-H15, C8-H13 and C9-H14 bonds
5	1197.31	122.318	Antisymmetric stretch of C4-C6-C7 coupled with bending mode of C8-H13, C11-H15 and C9-H14 bond
6	506.94	116.729	Out of plane bending of C7-N3-H12 bond (wagging), C6-C7, H13-C8, H15-C11 and H14-C9 bonds
7	1138.94	95.1121	Bending mode of C11-H15 bond and C9-H14 bond
8	1463.59	91.4056	Stretching mode of C9-C11 bond coupled with symmetric stretch of C10-C8-C4 and bending mode of H15-C11, H14-C9, and H12-N3 bond
9	3629.08	60.8597	Stretching mode of N3-H12 bond
10	1288.9	57.5583	Bending mode of C8-H13 and C11-H15 bond

Table 12 Vibrational spectra of IST-10A

S.NO	FREQ	INTENSITY	DESCRIPTION
1	1654.54	469.474	Stretching mode of C5-C9 bond coupled with antisymmetric stretch of C10-C8-C4 and bending mode of C9-H14, C8-H13, N3-H12
2	1814.24	418.061	Stretching mode of C6-O1 (major) bond and C7-O2 (minor) bond
3	1838.3	320.504	Stretching mode of C6-O1 (minor) bond and C7-O2 (major) bond
4	1320.01	160.493	Bending mode of N3-H12, C8-H13,C9-H14 coupled with stretching mode of H16-C11
5	1464.87	156.896	stretching mode of C8-C10, C9-C11, N3-C5 coupled with bending mode of N3-H12 and C8-H13
6	1177.59	153.714	Antisymmetric stretch of C7-C6-C4 coupled with bending mode of C4-C8-C10 bond (scizzoring) and C9--H14 bond
7	1150.43	123.441	Stretching mode of N3-C7 bond coupled with bending mode of C9-H14, C8-H13 and N3-H12
8	509.99	100.926	out of plane bending (wagging) mode of C7-N3-H12
9	1499.85	71.9901	Symmetric stretch of C9-C11-C10 and C8-C4-C5 coupled with bending mode of C9-H14, C8-H13 and N3-H12

10	3628.04	66.74	Stretching mode of N3-H12 bond
11	1378.77	60.4444	Antisymmetric stretch of C9-C11-C10 coupled with stretching mode of C4-C8 and bending mode of N3-H12

Table 13 Vibrational spectra of IST-10B

S.NO	FREQ	INTENSITY	DESCRIPTION
1	1649.25	506.423	Antisymmetric stretch of C11-C9-C5 bond and C10-C8-C4 bond coupled with bending mode of C8-H13, C9-H14 and N3-H12 bonds
2	1814.63	474.501	Stretching mode of O1-C6 (major) and O2-C7 (minor)
3	1836.64	316.179	Stretching mode of O2-C7 (major) and O1-C6 (minor) coupled with bending mode of N3-H12
4	1173.62	182.546	Stretching mode of C4-C6 bond coupled with in plane bending mode (scizzoring) in C11-C9-C5 bond and C10-C8-C4 bond
5	1440.59	117.382	Stretching mode of C10-C8 and C11-C9 bonds coupled with bending mode of C8-H13, C9-H14 and N3-H12
6	1482.47	110.416	Symmetric stretching of C5-C4-C8 coupled with bending mode of H14-C9 and H13-C8
7	511.53	102.643	Bending mode of N3-H12
8	1110.08	83.2345	Stretching mode of C10-C11 bond coupled with bending mode of C8-H13 and C9-H14
9	3628	64.2756	Stretching mode of N3-H12
10	1292.08	53.1211	Antisymmetric stretching mode of C11-C10-C8, C5-C9-C11, C8-C4-C5 coupled with bending mode of N3-H12 and C8-H13

Table 14 Vibrational spectra of IST-10C

S.NO	FREQ	INTENSITY	DESCRIPTION
1	1645.87	536.872	Antisymmetric stretch of C10-C8-C4 bond and C5-C9-C11 bond coupled with bending mode of N3-H12, C9-H14 and C8-H13 bond
2	1814.53	499.214	Stretching mode of O1-C6 bond (major) and O2-C7 bond (minor)
3	1836.4	315.336	Stretching mode of O2-C7 bond (major) and O1-C6 bond (minor) coupled with bending mode of N3-H12 bond
4	1172.05	188.801	Antisymmetric stretch of C7-C6-C4 coupled with bending mode of N3-H12 bond and C5-C4-C8 bond (In plane) and C5-C9-C11 bond (In plane)
5	1479.84	115.713	Symmetric stretch of C10-C11-C9 and C5-C4-C8 coupled with bending mode of C9-H14 and C8-H13 bond
6	1435.33	112.785	Stretching mode of C8-C10 bond and C11-C9 bond coupled with bending mode of C8-H13, C9-H14 and N3-H12 bonds
7	510.31	102.428	Out of plane bending of N3-H12 bond and O2-C7-N3 bond and O1-C6-C4 bonds (wagging)
8	3628.17	63.2277	Stretching mode of N3-H12 bond
9	1101.03	58.8693	Symmetric stretch of C10-C11-C9 bond coupled with bending mode of C8-H13 bond and C9-H14 bond

Table 15 Vibrational spectra of IST-10D

S.NO	FREQ	INTENSITY	DESCRIPTION
1	1819.71	452.674	Stretching mode of O1-C6 (major) and O2-C7 (minor)
2	1838.61	304.738	Stretching mode of O1-C6 (minor) and O2-C7 (major) coupled with bending mode of N3-H12
3	1493.86	266.858	Stretching mode of C8-C10, C9-C11, C4-C5 and C5-N3 coupled with bending mode of C11-H14 and C8-H13
4	1668.39	213.996	Stretching mode of C5-C9 and C4-C8-C10 (antisymmetric) coupled with bending mode of N3-H12 and C8-H13 bond
5	1308.86	161.116	Stretching mode of C10-C11, C5-C9, C4-C8 and C9-F16 coupled withbending mode of N3-H12 and C8-H13
6	1224.34	127.898	Stretching mode of C6-C4 coupled with bending mode of N3-H12, C11-H14, C5-C4-C8 (scizzoring), C8-C10-C11 (scizzoring), C10-C11-C9 (scizzoring)
7	1158.2	123.916	Stretching mode of N3-C7 coupled with bending mode of C8-H13, C11-H14, N3-H12 and C8-C4-C5 (Scizzoring)

8	490.05	95.318	Bending mode of N3-H12
9	3631.67	85.5257	Stretching mode of N3-H12
10	1397.7	52.5453	Bending mode of N3-H12, C11-H14, C5-C9-C11 (Scizzoring) coupled with antisymmetric stretch of C11-C10-C8, C10-C8-C4

Table 16 Vibrational spectra of IST-10E

S.NO	FREQ	INTENSITY	DESCRIPTION
1	1819.2	478.988	Stretching mode of C6-O10 (major) and C7-O20 (minor)
2	1838.8	306.499	Stretching mode of C6-O10 (minor) and C7-O20 (major) coupled with bending mode of N3-H12
3	1479.1	283.53	Stretching mode of C10-C8 and N3-C5-C4 (antisymmetric) coupled with bending mode of C8-H13, C11-H14 and N3-H12
4	1647.52	238.189	Antisymmetric stretch of C10-C8-C4 and C11-C9-C5 coupled with bending mode of C8-H13 and N3-H12
5	1158.39	181.597	Stretching mode of N3-C7 coupled with bending mode of C8-H13, C11-H14 and N3-H12
6	1179.65	74.1172	Stretching mode of C9-Cl16, C10-Br15 and C4-C5 coupled with bending mode of C11-H14
7	3626.21	71.2865	Stretching mode of N3-H12
8	486.05	63.66	Out of plane bending of N3-H12, C11-C9-Cl16, C5-C9-Cl16
9	1294.27	57.9793	Antisymmetric stretch of C4-C8-C10, C8-C10-C11, C10-C11-C9, C11-C9-C5, C9-C5-C4, C5-C4-C8 coupled with bending mode of N3-H12, C8-H13
10	530	51.8875	Out of plane bending of O20-C7-N3 (wagging), C7-N3-H12 (wagging), O10-C6-C7 (wagging), O10-C6-C4 (wagging), C9-C5-C4 (twisting), C9-C11-H14 (twisting), Cl16-C9-C11 (wagging), C4-C8-H13 (twisting), C7-C6-C4 (twisting)
11	1287.66	50.4373	Stretching mode of C11-C9 and N3-C7-C6 (antisymmetric) coupled with in plane bending of C11-H14, C8-H13, C5-N3-C7 (scizzoring)

Table 17 Vibrational spectra of IST-10F

S.NO	FREQ	INTENSITY	DESCRIPTION
1	1818.8	496.081	Stretching mode of C6-O10 (major) and C7-O20 (minor)
2	1837.61	298.153	Stretching mode of C6-O10 (minor) and C7-O20 (major) coupled with bending mode of N3-H12
3	1475.79	284.944	Stretching mode of C10-C8, C5-C9-C11 (Symmetric), C4-C5-C9 (Symmetric), C4-C5-N3 (Antisymmetric) coupled with bending mode of N3-H12, C8-H13, C11-H14
4	1643.55	245.511	Stretching mode of C10-C8-C4 (Antisymmetric), C5-C9-C11 (Antisymmetric) coupled with bending mode of C8-H13 and N3-H12
5	1157.6	224.576	Stretching mode of N3-C7 coupled with bending mode of C8-H13, N3-H12 and C11-H14
6	527.47	75.903	Out of plane bending mode of H12-N3-C7 (wagging), O20-C7-C6 (wagging), O10-C6-C4 (wagging), C4-C8-H13 (twisting), Br16-C9-C5 (wagging), C11-C9-C5 (wagging), N3-C7-O20 (wagging), C7-C6-O10 (wagging), C5-C4-C6 (wagging), C4-C5-C9 (twisting), H14-C11-C9 (twisting), C8-H13
7	1291.07	72.1581	Stretching mode of C11-C10-C8 (Antisymmetric), C4-C5-C9 (Antisymmetric), C8-C4-C5 (Antisymmetric), C9-C11-C10 (Antisymmetric), C5-C9-C11 (Antisymmetric), C10-C8-C4(Antisymmetric), C7-N3 coupled bending mode of N3-H12, C8-H13 and C11-H14
8	3620.11	66.4323	Stretching mode of N3-H12

Conclusion

Dibromoisatin derivatives exhibit a unique combination of chemical stability, reactive electronic properties, and favorable thermodynamics, which are likely to contribute their anticancer activity. The insights into their molecular behavior offer a foundation for understanding their mechanisms of action and for further development and optimization as anticancer agents. Dibromoisatin derivatives are characterized by their stability, which is crucial for their biological activity. The stability, influenced by the keto conformer, ensures that these compounds can interact effectively with biological targets without premature degradation. The thermochemical analysis suggests that dibromo derivatives are thermodynamically stable enough to participate in biological reactions. Their formation and stability under physiological conditions are essential for their efficacy as anticancer agents. The analysis of electronic transitions and global reactivity parameters indicates that dibromo derivatives possess unique electronic properties that may contribute to their interaction with biological molecules. The alterations in HOMO-LUMO gap, electronegativity, and other electronic parameters suggest a capacity for electron transfer and interaction with biomolecules, which is essential for anticancer activity. The global reactivity parameters, including chemical potential and global softness, indicate that dibromoisatin derivatives have a higher tendency to undergo chemical reactions. This reactivity could be exploited in targeting cancer cells, possibly through mechanisms involving reactive oxygen species (ROS) generation or interaction with DNA. The UV-Vis spectroscopy data suggest that dibromoisatin derivatives have distinct absorption characteristics, which could be relevant for their detection, tracking, and even for therapeutic applications that involve light activation. The vibrational spectra analysis provides insights into the molecular interactions and structural integrity of dibromoisatin derivatives. These interactions could be key in binding to specific biological targets, such as enzymes or receptors involved in cancer cell proliferation. The combined effects of stability, electronic properties, and chemical reactivity underpin the potential mechanisms through which dibromoisatin derivatives exert their anticancer effects. These could include inducing apoptosis, inhibiting angiogenesis, or interfering with the cancer cell cycle. Future research should aim to elucidate the specific biological pathways influenced by these compounds and to explore their potential in clinical settings.

Acknowledgement

Authors are thankful to Shyama Prasad Vidyalaya Lodi Estate and Prof. Amit Kumar, Department of Chemistry, Dyal Singh College, University of Delhi for supporting this work

References

1. Ke, S.; Shi, L.; Yang, Z. Discovery of novel isatin–dehydroepiandrosterone conjugates as potential anticancer agents. Bioorg. Med. Chem. Lett. 2015, 25(20): 4628–4631.
2. Pawar, V.S.; Lokwani, D.K.; Bhandari, S.V.; Bothara, K.G.; Chitre, T.S.; Devale, T.L.; Modhave, N.S.; Parikh, J.K. Design, docking study and ADME prediction of Isatin derivatives as anti-HIV agents. Med. Chem. Res. 2011, 20(3): 370–380.

3. Abbas, S.Y.; Farag, A.A.; Ammar, Y.A.; Atrees, A.A.; Mohamed, A.F.; El-Henawy, A.A. Synthesis, characterization, and antiviral activity of novel fluorinated isatin derivatives. Mon. Fur Chem. 2013, 144(11): 1725–1733.
4. Liang, C.; Xia, J.; Lei, D.; Li, X.; Yao, Q.; Gao, J. Synthesis, in vitro and in vivo antitumor activity of symmetrical bis-Schiff base derivatives of isatin. Eur. J. Med. Chem. 2014, 74: 742–750.
5. Jarrahpour, A.; Sheikh, J.; El Mounsi, I.; Juneja, H.; Hadda, T. Ben Computational evaluation and experimental in vitro antibacterial, antifungal and antiviral activity of bis-Schiff bases of isatin and its derivatives. Med. Chem. Res. 2013, 22(3): 1203–1211.
6. Raj, R.; Biot, C.; Carrère-Kremer, S.; Kremer, L.; Guérardel, Y.; Gut, J.; Rosenthal, P.J.; Forge, D.; Kumar, V. 7-Chloroquinoline–isatin Conjugates: Antimalarial, Antitubercular, and Cytotoxic Evaluation. Chem. Biol. Drug Des. 2014, 83(5): 622–629.
7. Eggadi, V.; Kulandaivelu, U.; Sheshagiri, S.B.B.; Jupalli, V. Evaluation of Antioxidant, Antimicrobial and Anticancer activity of Thiazole Tagged IsatinHydrazones. J. Pharm. Chem. 2016, 3(2): 4-9.
8. Rajanarendar, E.; Ramakrishna, S.; Govardhan Reddy, K.; Nagaraju, D.; Reddy, Y.N. A facile synthesis, anti-inflammatory and analgesic activity of isoxazolyl-2,3-dihydrospiro[benzo[f]isoindole-1,30 -indoline]-20 ,4,9-triones. Bioorg. Med. Chem. Lett. 2013, 23: 3954–3958.
9. El-Faham, A.; Hozzein, W.N.; Wadaan, M.A.M.; Khattab, S.N.; Ghabbour, H.A.; Fun, H.-K.; Siddiqui, M.R. Microwave Synthesis, Characterization, and Antimicrobial Activity of Some Novel Isatin Derivatives. J. Chem. 2015, 716987-94
10. Mondal, P.; Jana, S.; Balaji, A.; Ramakrishna, R.; Kanthal, L.K. Synthesis of Some New Isoxazoline Derivatives of ChalconisedIndoline 2-one as a Potential Analgesic, Antibacterial and AnthelmimticAgents. J. Young Pharm. 2012, 4(1): 38–41.
11. Firke, S.; Cheke, R.; Ugale, V.; Khadse, S.; Gagarani, M.; Surana, S.B. Rationale design, synthesis, and pharmacological evaluation of isatin analogues as antiseizure agents. Lett. Drug Des. Discov. 2021, 18(12): 1146-64.
12. Hamaue N.; Yamazaki N.; Minami M.; Endo T.; Hirafuji M.; Monma Y. Effect of isatin, an endogenous MAO inhibitor, on acetylcholine and dopamine levels in the rat striatum. Biog. Amines. 1999, 15(3): 367–77.
13. Medvedev A.; Buneeva O.; Glover V. Biological Targets for Isatin and Its Analogues: Implications for Therapy. Biologics: targets & therapy. 2007, 1(2): 151–162.
14. Motzer R.J., Escudier B., Gannon A., Figlin R.A. Sunitinib: Ten Years of Successful Clinical Use and Study in Advanced Renal Cell Carcinoma. Oncologist. 2017, 22(1):41–52.
15. Prabhakara, C.T.; Patil, S.A.; Toragalmath, S.S.; Kinnal, S.M.; Badami, P.S. Synthesis, characterization and biological approach of metal chelates of some first row transition metal ions with halogenated bidentate coumarin Schiff bases containing N and O donor atoms. J. Photochem. Photobiol. B. 2016, 157: 1–14.
16. Zhao, D.; Chen, C.; Liu, H.; Zheng, L.; Tong, Y.; Qu, D.; Han, S. Biological evaluation of halogenated thiazolo[3,2-a]pyrimidin-3-one carboxylic acid derivatives targeting the YycG histidine kinase. Eur. J. Med. Chem. 2014, 87: 500–507.
17. Becke, A. D. A multicenter numerical integration scheme for polyatomic molecules. J. Chem. Phys. 1988, 88(4): 2547-2553.

18. Becke, A. D. Density-functional exchange-energy approximation with correct asymptotic behavior. Phys. Rev. A: At. Mol. Opt. Phys. 1988, 38(6): 3098-3100.

19. Vosko, S. H.; Wilk, L.; Nusair, M. Accurate spin-dependent electron liquid correlation energies for local spin density calculations: a critical analysis. Can. J. Phys. 1980, 58: 1200-1211.

20. Andersson, M. P.; Uvdal, P. New scale factors for harmonic vibrational frequencies using the B3LYP density functional method with the triple-ζ basis set 6-311+G(d,p). J. Phys. Chem. A 2005, 109(12): 2937-2941.

21. Glendening, E. D.; Reed, A. E.; Carpenter, J. E.; Weinhold, F. NBO Version 3.1, 2003.

22. Bauernschmitt, R.; Ahlrichs, R. Treatment of electronic excitations within the adiabatic approximation of time dependent density functional theory. Chem. Phys. Lett. 1996, 256(4-5): 454-464.

23. Casida, M. E.; Jamorski, C.; Casida, K. C.; Salahub, D. R. Molecular excitation energies to high-lying bound states from time-dependent density-functional response theory: characterization and correction of the time-dependent local density approximation ionization threshold. J. Chem. Phys. 1998, 108(11): 4439-4449.

24. Stratmann, R. E.; Scuseria, G. E.; Frisch, M. J. An efficient implementation of time-dependent densityfunctional theory for the calculation of excitation energies of large molecules. J. Chem. Phys. 1998, 109(19): 8218-8224.

25. M. J. Frisch, G. W. Trucks, H. B. Schlegel, G. E. Scuseria, M. A. Robb, J. R. Cheeseman, G. Scalmani, V. Barone, B. Mennucci, G. A. Petersson, H. Nakatsuji, M. Caricato, X. Li, H. P. Hratchian, A. F. Izmaylov, J. Bloino, G. Zheng, J. L. Sonnenberg, M. Hada, M. Ehara, K. Toyota, R. Fukuda, J. Hasegawa, M. Ishida, T. Nakajima, Y. Honda, O. Kitao, H. Nakai, T. Vreven, J. A. Montgomery, Jr., J. E. Peralta, F. Ogliaro, M. Bearpark, J. J. Heyd, E. Brothers, K. N. Kudin, V. N. Staroverov, R. Kobayashi, J. Normand, K. Raghavachari, A. Rendell, J. C. Burant, S. S. Iyengar, J. Tomasi, M. Cossi, N. Rega, J. M. Millam, M. Klene, J. E. Knox, J. B. Cross, V. Bakken, C. Adamo, J. Jaramillo, R. Gomperts, R. E. Stratmann, O. Yazyev, A. J. Austin, R. Cammi, C. Pomelli, J. W. Ochterski, R. L. Martin, K. Morokuma, V. G. Zakrzewski, G. A. Voth, P. Salvador, J. J. Dannenberg, S. Dapprich, A. D. Daniels, O¨ . Farkas, J. B. Foresman, J. V. Ortiz, J. Cioslowski, D. J. Fox, Gaussian 09, Version A.02; Gaussian, Inc.: Wallingford, CT, 2009.

26. Wolinski, K., Hinton, J. F. & Pulay, P. Efficient implementation of the gauge-independent atomic orbital method for NMR chemical shift calculations. J. Am. Chem. Soc. 1990,112(23): 8251-8260.